PHYSICAL REVIEW D **77,** 064005 (2008)

# Near extremal black hole entropy as entanglement entropy via $AdS_2/CFT_1$

Tatsuo Azeyanagi,* Tatsuma Nishioka,† and Tadashi Takayanagi‡

*Department of Physics, Kyoto University, Kyoto 606-8502, Japan*

(Received 4 January 2008; published 5 March 2008)

We point out that the entropy of (near) extremal black holes can be interpreted as the entanglement entropy of dual conformal quantum mechanics via $AdS_2/CFT_1$. As an explicit example, we study near extremal Banados-Teitelboim-Zanelli black holes and derive this claim from $AdS_3/CFT_2$. We also analytically compute the entanglement entropy in the two dimensional CFT of a free Dirac fermion compactified on a circle at finite temperature. From this result, we clarify the relation between the thermal entropy and entanglement entropy, which is essential for the entanglement interpretation of black hole entropy.

DOI: 10.1103/PhysRevD.77.064005 PACS numbers: 04.70.Dy, 04.50.Gh

## I. INTRODUCTION

The AdS/CFT [1] has been studied for almost ten years, and many interesting aspects of quantum gravity have been revealed. Even though the examples of $AdS_{d+1}/CFT_d$ with $d \geq 2$ have been explored in detail, the lowest dimensional case, $d = 1$, is still not well understood. The $AdS_2$ geometry appears as the near horizon limit of four or five dimensional extremal black holes (or black rings) [2–4]. Thus the microscopic explanation of Bekenstein-Hawking entropy of the extremal black holes [5,6] is expected to be directly related to the $AdS_2/CFT_1$ correspondence [1,7] (see [8] for a review).

The pure AdS spacetime $AdS_{d+1}$ with $d \geq 2$ has no entropy as is also clear from its dual $CFT_d$ at vanishing temperature. To obtain nonzero entropy, we need to consider an AdS black hole as the dual geometry. On the other hand, we expect nonzero entropy even for the pure $AdS_2$, since it is the near horizon limit of higher dimensional (near) extremal black holes. We also notice another special property of $AdS_2$, that the $AdS_{d+1}$ in the global coordinate has two (timelike) boundaries only when $d = 1$. The latter property is a major problem when discussing $AdS_2/CFT_1$ because the CFT lives on the boundary of AdS spacetime. So far, this issue has been neglected, and the $AdS_2$ space is considered to be dual to a single CFT with a large degeneracy. Though it is also natural to assume that there are two CFTs, taking into account the presence of two boundaries on $AdS_2$, there have been no arguments in this direction as far as the authors know.

In this paper, we would like to report progress in this direction owing to the recently found method of holographically computing entanglement entropy [9,10]. We point out that the above two exceptional properties of $AdS_2$ are closely related with each other. We present important evidence that there exist two systems of conformal quantum mechanics (CQM) on the boundaries of the $AdS_2$ and that they are entangled with each other as is speculated from the nonvanishing correlation functions between them computed holographically. Indeed, we will be able to show that the black hole entropy is exactly the same as the entanglement entropy of CQM if we assume the $AdS_2/CFT_1$ correspondence with this interpretation. This relation is true even if we take any higher derivative corrections into account. We can say that this progress is highly remarkable if we remember that the $AdS_2/CFT_1$ has been poorly understood and is still mysterious.

Even though our argument can be regarded as a generalization of the interpretation of AdS black holes in [11] via AdS/CFT, it is slightly different from it in the following way. For the (3D or higher dimensional) AdS black holes, its CFT dual is well established and it is possible to explicitly construct a dual entangled CFT state, from which we can compute its entanglement entropy directly as in [11]. On the other hand, in the $AdS_2$ case, we can perform a computation of entanglement entropy in the dual CFT only by using the recent holographic method[1] [9,10], as the formulation of the dual CFT is not clear at present.

The relation between the black hole entropy and entanglement entropy has been discussed for a long time, and historically this was the first motivation to make us consider the entanglement entropy in quantum field theory [14]. Later, it turned out that quantum corrections to Bekenstein-Hawking formula could be explained as the entanglement entropy [15,16]. In particular, when the entire gravity action is induced, the black hole entropy itself can be regarded as the entanglement entropy [16,17]. In these arguments, the black hole entropy is related to the entanglement entropy *in the quantum field theory in the same spacetime*. The corresponding interpretation from the viewpoint of AdS/CFT has been given in [18,19] (see also [20–22]). On the other hand, in our case, the black hole entropy is interpreted as the entanglement entropy *in CFT (or CQM) which lives on the boundary of the spacetime*.

*aze@gauge.scphys.kyoto-u.ac.jp
†nishioka@gauge.scphys.kyoto-u.ac.jp
‡takayana@gauge.scphys.kyoto-u.ac.jp

[1]This holographic method has also been applied to the analysis of the confining gauge theories [12,13].

 

Now, we usually identify the black hole entropy with the thermal entropy based on AdS/CFT. Thus in order to claim the equality between the black hole entropy and the entanglement entropy in general setups, we need to establish the relation between the thermal entropy and the entanglement entropy. To see that it indeed agrees with what we expect from the holographic viewpoint, we compute the entanglement entropy of a 2D free Dirac fermion at finite temperature with the spatial direction compactified as an explicit example. We finally obtain an analytical expression and are able to check this relation. This is the first analytic result on entanglement entropy with both the finite temperature and the finite size effects taken into account.[2] Also remarkably, in our setup the entanglement entropy depends on the detail of the 2D CFT, while the entanglement entropy at zero temperature or in the infinite system only depends on the central charge of CFT [23,24].

This paper is organized as follows: In Sec. II we explain the holographic computation of entanglement entropy via the AdS/CFT duality. We also present new evidence of this relation in Banados-Teitelboim-Zanelli (BTZ) black holes. In Sec. III, we give a general argument to show the equivalence between the black hole entropy and the entanglement entropy via $AdS_2/CFT_1$. In Sec. IV, we investigate near extremal BTZ black holes in order to derive our claim from $AdS_3/CFT_2$. In Sec. V, we analytically compute the entanglement entropy of a 2D free Dirac fermion at finite temperature with the spacial direction compactified. In Sec. VI, we draw a conclusion and discuss future problems.

## II. HOLOGRAPHIC ENTANGLEMENT ENTROPY AND BTZ BLACK HOLES

The main purpose of this paper is to understand the $AdS_2/CFT_1$ better by uncovering the relation between the black hole entropy and the entanglement entropy in $CFT_1$. However, it is quite useful to learn a general holographic prescription of computing entanglement entropy from the AdS/CFT correspondence. This is because the dual CFT in $AdS_2/CFT_1$ is not understood well, and we need to employ a holographic computation of the entanglement entropy[3] for $CFT_1$. We will apply this general method to the $AdS_2/CFT_1$ setup in the next section. Also, in a particular case of $AdS_2$, background in string theory can be embedded into a rotating BTZ black hole, which is asymptotically $AdS_3$ as we will see.

Motivated by this, we will explain the general holographic computation of the entanglement entropy [9] in this section. In particular, we study the example of BTZ black holes and its $CFT_2$ dual based on the $AdS_3/CFT_2$, and present a new result. This gives further evidence that the general prescription in [9] correctly reproduces the black hole entropy as the entanglement entropy. Also, the entropy of BTZ black holes is closely related to the entropy of extremal black holes, which is the main topic of this paper as we will see later.

### A. Holographic entanglement entropy

Consider a CFT and divide the space manifold of the CFT into two parts, $A$ and $B$. This factorizes the total Hilbert space into a direct product of two Hilbert spaces, $H_A \otimes H_B$. The entanglement entropy is defined by the von Neumann entropy $S_A = -\mathrm{Tr}\rho_A \log\rho_A$ for the reduced density matrix $\rho_A$. The reduced density matrix $\rho_A$ is defined by tracing out the density matrix over $H_B$ i.e. $\rho_A = \mathrm{Tr}_B\rho$. We have infinitely many such quantities for various choices of $A$.

Now we would like to compute the entanglement entropy from the AdS/CFT correspondence. We assume a setup where a $AdS_{d+2}$ space with the Newton constant $G_N^{(d+2)}$ is dual to a $CFT_{d+1}$. The CFT lives on the boundary of AdS. Then the general holographic prescription in [9] computes the entanglement entropy as the area of the minimal surface at a constant time,

$$S_A = \frac{\mathrm{Area}(\gamma_A)}{4G_N^{(d+2)}}, \tag{2.1}$$

where $\gamma_A$ is the (unique) minimal surface in $AdS_{d+2}$ whose boundary coincides with the boundary of the region $A$. A simple proof of this claim has been given in [25]. Notice that this formula assumes the supergravity approximation of the full string theory.

### B. Application to BTZ black holes

As a particular example, which is also relevant to the discussions in the next section, let us consider the BTZ black holes [26], whose metric is given as follows:

$$ds^2 = -\frac{(r^2 - r_-^2)(r^2 - r_+^2)}{R^2 r^2}dt^2 + \frac{R^2 r^2}{(r^2 - r_-^2)(r^2 - r_+^2)}dr^2 + r^2\left(d\phi + \frac{r_+ r_-}{Rr^2}dt\right)^2. \tag{2.2}$$

The boundary of BTZ black holes at a fixed time is a circle because $\phi$ has the periodicity $\phi \sim \phi + 2\pi$. The entanglement entropy is defined by dividing this circle into two parts, $A$ and $B$. We specify the size of $A$ by the angle $\Delta\phi = 2\pi L$, while the size of $B$ becomes $\Delta\phi = 2\pi(1 - L)$.

If we apply the holographic formula (2.1) to BTZ black holes, $\mathrm{Area}(\gamma_A)$ is equal to the geodesic length between the two endpoints of $A$ inside the bulk space. This holographic computation leads to the following prediction [9]:

[2]Since this result may also be interesting for those who are interested in other subjects, we arranged Sec. V such that it is readable for anyone who is familiar with 2D CFT.

[3]Again, please distinguish this entanglement entropy in $CFT_1$ from the entanglement entropy in $AdS_2$.

$$S_A = \frac{c}{3}\log\left[\frac{\beta}{\pi a}\sinh\left(\frac{\pi L}{\beta}\right)\right], \tag{2.3}$$

where $c$ is the central charge of the dual $CFT_2$ and $\beta$ is the inverse temperature of the black hole. This agrees with the result in [24], which computes the entanglement entropy in any 2D finite temperature CFT when the size $L$ is small. However, when $L$ is large, the formula (2.3) is no longer correct, as will be clear from the holographic consideration discussed just below.

At high temperature, the geodesic winds around the black hole horizon as $L$ becomes large [Fig. 1(a)]. When the region $A$ covers most of the boundary ($L = 1 - \epsilon$ with $\epsilon \ll 1$), the disconnected surface [Fig. 1(c)] gives smaller area than[4] the connected surface [Fig. 1(b)]. Thus the disconnected surface consists of the total black hole horizon and the geodesic extending to the boundary. Taking the $\epsilon \to 0$ limit, this leads to

$$S_A(L = 1 - \epsilon) = S_{\rm BH} + S_A(L = \epsilon), \tag{2.4}$$

where $S_{\rm BH}$ is the black hole entropy. The relation (2.4) offers an important way to extract the black hole entropy from the entanglement entropy of $CFT_2$.

Therefore it is very important to confirm (2.4) from the CFT side without assuming AdS/CFT. Indeed in Sec. III C we will show this is indeed true for a particular CFT. There, we consider the example[5] of free fermion CFT since it turns out to be possible to compute the entanglement entropy analytically and show this relation as in (5.22).

In this way we have been able to understand well the BTZ black hole entropy from the viewpoint of entanglement entropy. This gives further evidence of $AdS_3/CFT_2$. In the next sections, we would like to proceed to another important class of black holes, i.e. the ones whose near horizon geometry includes the $AdS_2$.

[4]Remember that, when the temperature is nonvanishing but is not high enough, the AdS/CFT claims that the dual gravity description is given by the path integral over infinitely many geometries as in [27,28]. Thus our results, such as (5.17) and (5.24), which are correct for any values of $\beta$, should include such a sum over geometries.

[5]In this subsection, we have proceeded by pretending that the free Dirac fermion system has its AdS dual. We believe this assumption is not crucial because the property (5.19) should be true for any 2D CFT. It is well known that the IIB string on $AdS_3 \times S^3 \times M$ ($M = K3$ or $T^4$) is dual to the 2D (4, 4) superconformal field theory defined by the symmetric orbifolds $\mathrm{Sym}(M)^N$. Thus it will be an interesting future problem to extend our calculations of entanglement entropy to the ones in symmetric orbifolds $\mathrm{Sym}(M)^N$ and see that the result can explicitly be interpreted as the sum over geometries.

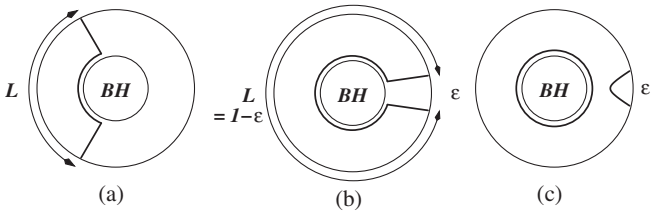


FIG. 1. Holographic picture of the entanglement entropy. (a) The length of the geodesic $\gamma_A$ whose boundary coincides with $\partial A$ gives the holographic entanglement entropy of region $A$. (b) As region $A$ covers a large part of the boundary, the geodesic wraps the black hole horizon. (c) When region $A$ covers almost all the boundary, we have another candidate for $\gamma_A$ which consists of two disconnected curves. The one wraps the black hole horizon and the other extends to the boundary. The former has a finite length, while the latter is infinitely long, $\sim \frac{c}{3} \times \log(\epsilon/a)$.

## III. BLACK HOLE ENTROPY AS ENTANGLEMENT ENTROPY AND $AdS_2/CFT_1$

### A. $AdS_2$ from the near horizon limit of the extremal black hole

The metric of a 4D charged black hole looks like

$$ds^2 = -\frac{(r-a_+)(r-a_-)}{r^2}dt^2 + \frac{r^2}{(r-a_+)(r-a_-)}dr^2 + r^2 d\Omega_2^2, \tag{3.1}$$

where we assumed $a_+ \geq a_-$. The Bekenstein-Hawking entropy is given by

$$S_{\rm BH} = \frac{A}{4G_N^{(4)}} = \frac{\pi a_+^2}{G_N^{(4)}}. \tag{3.2}$$

The extremal black hole corresponds to the special choice of the parameter $a_+ = a_-$. In this case, if we define $u = r - a_+$, the near horizon metric becomes

$$ds^2 = -\frac{u^2}{a_+^2}dt^2 + a_+^2\frac{du^2}{u^2} + a_+^2 d\Omega_2^2, \tag{3.3}$$

i.e. $AdS_2$ in the Poincare coordinate times $S^2$.

More generally, it is possible to obtain $AdS_2 \times S^2$ when the black hole is near extremal, $\frac{a_+ - a_-}{a_+} \ll 1$ [29]. In this case, the dual ground state in $AdS_2$ is heated up into a thermal state so that its temperature is proportional to $a_+ - a_-$. As we will see in the last part of the next section, the extremal black hole $a_+ = a_-$ behaves differently from the near extremal one, especially in the global structure of the spacetime. Below we mostly consider the extremal limit of the near extremal black hole instead of the extremal one itself.

As is well known, the $AdS_2$ in the global coordinate,

$$ds^2 = a_+^2\frac{-d\tau^2 + d\sigma^2}{\cos^2\sigma}, \tag{3.4}$$

has a significant difference from the higher dimensional AdS spaces in that it has two timelike boundaries at $\sigma = \pm\frac{\pi}{2}$. Thus it is natural to expect that the theory is dual to two copies of conformal quantum mechanics, CQM1 and CQM2, living on the two boundaries via $AdS_2/CFT_1$. In the next section, by considering 5D (near) extremal black holes, we will give an explicit example of $AdS_2/CFT_1$ duality, which supports this interpretation.

In the case of 4D extremal black holes, the systematic construction of dual CQM has not been established. There are some specific examples whose dual quantum mechanics is understood [30–32]. Instead of the detailed review of each example, we would like to briefly give a sketchy explanation since the detail is not necessary for our purpose. Consider the setup of type IIA string compactified on a Calabi-Yau 3-fold with D0-branes and D4-branes. We specify the number of D0-branes and D4-branes wrapped on the 4-cycle $\alpha_A$ by $q_0$ and $p^A$. This configuration leads to a macroscopic Bogomol'nyi-Prasad-Sommerfield (BPS) black hole with the entropy $S = 2\pi\sqrt{q_0 D}$ in a large charge limit, where $D = \frac{1}{6}C^{ABC}p_A p_B p_c$ in terms of the intersection number $C^{ABC}$ [33]. In the near horizon limit, the geometry $AdS_2 \times S^2$ is realized. In this setup, the dual quantum mechanics is described by a supersymmetric sigma model whose target space is the symmetric product $\mathrm{Sym}(P^{q_0})$ of a certain manifold $P$ [30]. This manifold $P$ represents the effective geometry of the D4-brane world volume probed by a D0-brane. The number of ground states $d(q_0)$ of this model is equal to the number of cohomology of the symmetric product $\mathrm{Sym}(P^{q_0})$. We can apply the orbifold formula as usual to count $d(q_0)$ [5,34]. This turns out to be equivalent to the counting of left-moving states of a two dimensional CFT at level $q_0$ with the central charge $c_L = 6D$ [30,33]. This reproduces $S = \log d(q_0) = 2\pi\sqrt{q_0 D}$. In this setup, we can regard the pair CQM1 and CQM2 as the two copies of the symmetric product quantum mechanics.

### B. Holographic computation of entanglement entropy

Since there are two CQMs, it is natural to ask if there are any correlations between them. We can compute from the standard bulk-boundary relation [35] the two-point function between $\mathcal{O}_1$ in $CFT_1$ and $\mathcal{O}_2$ in $CFT_2$ as follows [we assume the global $AdS_2$ (3.4)]:

$$\langle \mathcal{O}_1(\tau_1)\mathcal{O}_1(\tau_2)\rangle = \frac{1}{[\sin(\frac{\tau_1-\tau_2}{2})]^{2h}}, \tag{3.5}$$

$$\langle \mathcal{O}_1(\tau_1)\mathcal{O}_2(\tau_2)\rangle = \frac{1}{[\cos(\frac{\tau_1-\tau_2}{2})]^{2h}}, \tag{3.6}$$

where $h$ is the conformal dimension of the operator $\mathcal{O}_{1,2}$.

At first, one may think they are decoupled because the CQM1 and CQM2 are disconnected. However, as the nonvanishing two-point functions show, AdS/CFT predicts that they are actually correlated. A similar puzzle has been raised in [36] in the context of AdS wormholes. Indeed the following discussion is closely related to the holographic computation of entanglement entropy in AdS wormholes [10].

In this paper we would like to claim that CQM1 and CQM2 are actually quantum mechanically entangled with each other and that this is the reason why we get the nonvanishing correlators. To show that the two CFTs are entangled, we need to compute the entanglement entropy and check that it is nonzero. Below we would like to calculate the entanglement entropy holographically.

The holographic formula (2.1) is expected to be true in general AdS space. If we apply it to our $AdS_2$ setup [i.e. $d = 0$ in (2.1)], we naturally find

$$S_{\mathrm{ent}} = \frac{\mathrm{Area}(\gamma_A)}{4G_N^{(2)}} = \frac{1}{G_N^{(2)}}. \tag{3.7}$$

This is because the minimal surface now becomes a point. Below we will give a clearer derivation of (3.7) based on the AdS/CFT.

The Hilbert spaces of CQM1 and CQM2 are denoted by $H_1$ and $H_2$. The total Hilbert space looks like $H_{\mathrm{tot}} = H_1 \otimes H_2$. We define the reduced density matrix from the total density matrix $\rho_{\mathrm{tot}}$,

$$\rho_1 = \mathrm{Tr}_{H_2}\rho_{\mathrm{tot}}, \tag{3.8}$$

by tracing over the Hilbert space $H_2$. This is the density matrix for an observer who is blind to CQM2. It is natural to assume that $\rho_{\mathrm{tot}}$ is the one for a pure state.

The entanglement entropy for CQM1, when we assume that the opposite part CQM2 is invisible for the observer in CQM1, is defined by

$$S_{\mathrm{ent}} = \mathrm{Tr}[-\rho_1 \log\rho_1]. \tag{3.9}$$

We can obtain this by first computing $\mathrm{Tr}(\rho_1)^n$, taking the derivative with respect to $n$ and finally setting $n = 1$. In the path-integral formalism of quantum mechanics, $\rho_1$ and $\mathrm{Tr}(\rho_1)^n$ are computed as in Fig. 2 (we perform the path

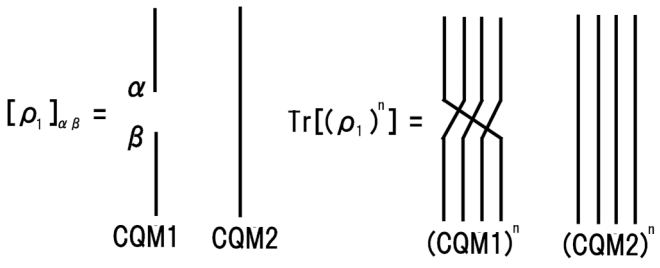


FIG. 2. The calculation of reduced density matrix $\rho_1$. In the path-integral formalism, the wave function is described by the path integral from $t = -\infty$ to a given time (say, $t = 0$). We can compute the reduced density matrix and the trace of its $n$th power, as we show in this figure, employing the path-integral formalism.

integral along the thick lines; $\alpha$ and $\beta$ are the boundary conditions).

By using the bulk-boundary relation of AdS/CFT [35], we can compute the entanglement entropy holographically as on the right side of Fig. 3. The dual geometry is the $n$-sheeted Riemann surface [9]. Though our derivation below is along the lines of the argument in [25] for $\mathrm{AdS}_{d\geq 3}$, which proves the claim in [9] via the bulk-to-boundary relation [35], our example is more nontrivial as it includes two boundaries. Also, it is closely related[6] to the conical defect argument of black hole entropy (see e.g. [17,37]).

Here we are considering a Euclidean metric. The cut should end on a certain point in the bulk because there should not be any cut on the opposite boundary, which is first traced out. Notice that the presence of two boundaries in $\mathrm{AdS}_2$ plays a crucial role in this holographic computation. We would get the vanishing entropy if we were to start with the spacetime which has a single boundary, such as the Poincare metric of $\mathrm{AdS}_2$.

Now we remember the Einstein-Hilbert action in the Euclidean space,

$$I_{\mathrm{EH}} = -\frac{1}{16\pi G_N^{(2)}} \int dx^2 \sqrt{g}(R + \Lambda). \tag{3.10}$$

The cosmological constant $\Lambda$ is not important since it is extensive and will vanish in the end of the entropy computation. In the $n$-sheeted geometry we find $S_{\mathrm{EH}} = \frac{n-1}{4G_N^{(2)}}$ in the Euclidean formalism because the curvature behaves like a delta function, $R = 4\pi(1-n)\delta^2(x)$ (see e.g. [25,37]). The entanglement entropy is obtained as follows:

$$S_{\mathrm{ent}} = -\frac{\partial}{\partial n} \log(e^{-I_{\mathrm{EH}} + n I_{\mathrm{EH}}^{(0)}})|_{n=1} = \frac{1}{4G_N^{(2)}}, \tag{3.11}$$

where $S_{\mathrm{EH}}^{(0)}$ is the value of the Einstein-Hilbert action of a single sheet in the absence of the cut (or negative deficit angle).

Finally, it is trivial to see that

$$S_{\mathrm{ent}} = S_{\mathrm{BH}}, \tag{3.12}$$

because $\frac{1}{G_N^{(2)}} = \frac{4\pi r_+^2}{G_N^{(4)}}$. This means that the entanglement between CQM1 and CQM2 is precisely the source of the 4D (near) extremal black hole entropy. The same argument can be applied to any $d$ dimensional black holes or black rings whose horizons are of the form $\mathrm{AdS}_2 \times M_{d-2}$, where $M_{d-2}$ is a compact manifold such as $S^{d-2}$.

Recently, it has been shown that extremal (rotating) black holes always have the $SO(2,1)$ symmetry in the near horizon limit [2–4]. For example, the near horizon geometry of a four dimensional extremal Kerr black hole is given by a warped product of $\mathrm{AdS}_2$ and a two dimensional manifold [38]. Our argument in this subsection can be applied to such a warped $\mathrm{AdS}_2$ case.

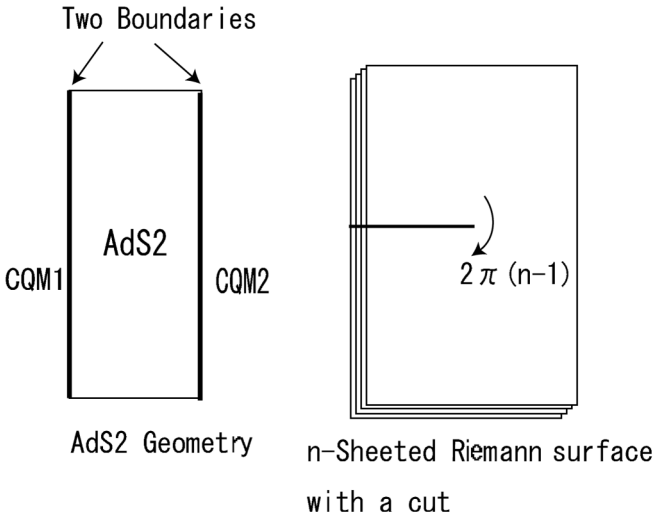


FIG. 3. In the left figure, we show the geometry of $\mathrm{AdS}_2$ in the global coordinate. It has two boundaries separated by the bulk spacetime. The right figure represents the 2D spacetime, which is dual to the computation $\mathrm{Tr}(\rho_1)^n$.

### C. Higher derivative corrections

Moreover, we can take curvature corrections into account. We assume that the near horizon geometry is of the form $\mathrm{AdS}_2 \times S^{d-2}$. Even though we start with the Lagrangian $\mathcal{L}$ that includes the curvature tensor $R_{\mu\nu\rho\sigma}$ and its covariant derivatives, we can neglect the covariant derivative of curvature tensors because the near horizon geometry has constant curvature. In this case, the black hole entropy with the curvature corrections is given by Wald's formula [39,40],

$$S_{\mathrm{BH}} = -2\pi \int_{\mathcal{H}} \sqrt{h} \frac{\partial \mathcal{L}}{\partial R_{\mu\nu\rho\sigma}} \epsilon_{\mu\nu}\epsilon_{\rho\sigma}, \tag{3.13}$$

where $\epsilon_{\mu\nu} = \xi_\mu \eta_\nu - \xi_\nu \eta_\mu$ by using the Killing vector $\xi_\mu$ of the Killing horizon and its normal $\eta_\nu$, normalized such that $\xi \cdot \eta = 1$; $\mathcal{H}$ represents the horizon and $h$ is the metric on it.

For example, in the ordinary Einstein-Hilbert action $I = -\frac{1}{16\pi G_N} \int dx^d \sqrt{g} R = -\int dx^d \sqrt{g} \mathcal{L}$, we reproduce the standard result

$$S = \frac{A_H}{8G_N} \epsilon_{\mu\nu}\epsilon_{\rho\sigma} g^{\mu\rho} g^{\nu\sigma} = \frac{A_H}{4G_N}, \tag{3.14}$$

where $A_H$ is the horizon area.

Now we would like to compare the Wald entropy with the entanglement entropy computed holographically via $\mathrm{AdS}_2/\mathrm{CFT}_1$. We consider the $n$-sheeted $\mathrm{AdS}_2$ (times the

[6]Notice that in these arguments the authors consider the entanglement entropy for the *total spacetime* of nonextremal black holes, while in our argument we consider the entanglement entropy for *the boundary of* the extremal black hole geometry.

same $S^{d-2}$), where the Riemann tensor behaves as follows [37]:

$$R_{abcd} = R^{(0)}_{abcd} + 2\pi(1-n)\cdot(g_{ac}g_{bd} - g_{ad}g_{bc})\cdot\delta_H. \tag{3.15}$$

Here $\delta_H$ is the delta function localized at the (codimension two) horizon; $R^{(0)}_{abcd}$ represents the constant curvature contribution from the cosmological constant. $a$, $b$ run the coordinate in the $AdS_2$. Notice also that, if we employ the relation $g_{ab} = \xi_a\eta_b + \xi_b\eta_a$, we obtain

$$\epsilon_{ab}\epsilon_{cd} = -(g_{ac}g_{bd} - g_{ad}g_{bc}). \tag{3.16}$$

Now we consider the perturbative expansions of the Lagrangian with respect to the (delta functional) deviation of $R_{abcd}$ from $R^{(0)}_{abcd}$. Then the quadratic and higher order terms do not contribute since $\lim_{n\to 1}\frac{d}{dn}(1-n)^d = 0$ for $d \geq 2$. Therefore, we can find

$$\begin{aligned} I_n &= -\log Z_n \\ &= -\int dx^d\sqrt{-g}\,\frac{\partial\mathcal{L}}{\partial R_{abcd}}(-\epsilon_{ab}\epsilon_{cd})2\pi(1-n)\delta_H \\ &= 2\pi(1-n)\int_H\sqrt{h}\,\frac{\partial\mathcal{L}}{\partial R_{abcd}}\epsilon_{ab}\epsilon_{cd}. \end{aligned} \tag{3.17}$$

Thus this agrees with Wald's formula,

$$\begin{aligned} S_{\text{ent}} &= -\frac{\partial}{\partial n}\log Z_n\Big|_{n=1} = -2\pi\int_H\sqrt{h}\,\frac{\partial\mathcal{L}}{\partial R_{\mu\nu\rho\sigma}}\epsilon_{\mu\nu}\epsilon_{\rho\sigma} \\ &= S_{\text{BH}}. \end{aligned} \tag{3.18}$$

### D. Towards holography in flat spacetime

For general nonextremal black holes,

$$ds^2 = -\frac{(r-r_+)(r-r_-)}{r^2}dt^2 + \frac{r^2}{(r-r_+)(r-r_-)}dr^2 + r^2d\Omega^2, \tag{3.19}$$

we obtain a Rindler space in the near horizon limit $r \to r_+(>r_-)$. The global extension of the Rindler space is clearly the two dimensional Minkowski spacetime $R^{1,1}$. Thus we cannot relate it to the AdS/CFT correspondence.

If we associate two quantum mechanical systems, however, to two timelike curves situated on the left and right sides of $R^{1,1}$, then we can obtain the same equality as (3.12). This suggests that the flat Minkowski spacetime may admit its holographic description. It also has a natural higher dimensional extension by expressing the $R^{1,d}$ metric as $ds^2 = dr^2 + r^2ds^2_{\text{dS}_d}$, where $ds^2_{\text{dS}_d}$ is the metric of the $d$ dimensional de Sitter space.

## IV. THE $AdS_2/CFT_1$ DUALITY FROM 5D NEAR EXTREMAL BLACK HOLES

In the previous section we have argued that the black hole entropy of (near) extremal black holes, whose near horizon geometry includes an $AdS_2$ factor, is equal to the entanglement entropy of two dual CQMs, including quantum corrections. We confirmed this claim by assuming the $AdS_2/CFT_1$. To obtain a complete proof, we need to explicitly present a general construction of the entangled pair of CQMs. In the 4D black hole cases, this is not straightforward because the CQM dual to $AdS_2$ is not well understood at present.

Instead, in this section we would like to examine a concrete example of $AdS_2/CFT_1$ which is obtained from the near extremal limit of nonrotating 5D black holes. Equally, we can regard this as a dimensional reduction of $AdS_3/CFT_2$ as first pointed out in [7] since the near horizon geometry of 5D near extremal black holes is a rotating BTZ black hole [26,41] (see also [27]).

### A. Near extremal BTZ black hole from 5D black holes

Consider a 5D black hole which is obtained from the type IIB background with $Q_1$ D1-branes and $Q_5$ D5-branes wrapped on $T^4 \times S^1$ with Kaluza-Klein momentum $N$ in the $S^1$ direction. In the near horizon limit, the metric becomes [6]

$$\begin{aligned} \frac{ds^2}{\alpha'} = \frac{U^2}{l^2}(-dt^2 + (dx^5)^2) + \frac{U_0^2}{l^2}(\cosh\sigma dt + \sinh\sigma dx^5)^2 \\ + \frac{l^2}{U^2 - U_0^2}dU^2 + l^2(d\Omega_3)^2 + \sqrt{\frac{Q_1}{vQ_5}}dx_i^2. \end{aligned} \tag{4.1}$$

Via a coordinate transformation we can show that this geometry is equivalent to [27]

$$(\text{BTZ black hole})_3 \times S^3 \times T^4. \tag{4.2}$$

The metric of the rotating BTZ black hole [26,41] is given by (2.2). The explicit coordinate transformation is given by

$$\begin{aligned} &t \to bt, \qquad x^5 \to bR\phi, \\ &(U^2 + U_0^2\sinh^2\sigma) \to \frac{r^2}{b^2}, \quad \text{for } \forall b \end{aligned} \tag{4.3}$$

and the new parameters are defined as $R = l$, $r_+ = bU_0\cosh\sigma$, $r_- = bU_0\sinh\sigma$. We can take $\phi \sim \phi + 2\pi$ if we choose $b = R_5/R$, where $R_5$ is the radius of $x_5$.

This BTZ geometry (2.2) can also be obtained from a Lorentzian orbifold of the pure $AdS_3$ space,

$$ds^2 = R^2\frac{dy^2 + dw_+dw_-}{y^2}. \tag{4.4}$$

They are related by the coordinate transformation

$$w_\pm = \sqrt{\frac{r^2 - r_+^2}{r^2 - r_-^2}} e^{(r_+ \pm r_-/R)(\pm(t/R)+\phi)}, \qquad y = \sqrt{\frac{r_+^2 - r_-^2}{r^2 - r_-^2}} e^{(r_+/R)\phi + (r_-/R^2)t}. \tag{4.5}$$

The periodicity of $\phi$ (i.e. $\phi \sim \phi + 2\pi$) leads to the identification

$$w_+ \sim e^{4\pi^2 T_L} w_+, \qquad w_- \sim e^{4\pi^2 T_R} w_-, \qquad y \sim e^{2\pi^2 (T_L + T_R)} y, \tag{4.6}$$

where $T_L = \frac{r_+ + r_-}{2\pi R}$ and $T_R = \frac{r_+ - r_-}{2\pi R}$ represent the left- and right-moving temperature of the dual 2D CFT. The central charge of dual CFT is given by $c = \frac{3R}{2G_N^{(3)}}$, and its density matrix looks like

$$\rho = e^{-(L_0/T_L) - (\bar{L}_0/T_R)}, \tag{4.7}$$

using the left- and right-moving energy, $L_0$ and $\bar{L}_0$.

In the extremal case $r_+ = r_-$, we need another coordinate transformation defined by

$$w_+ = \frac{R}{2r_+} e^{(2r_+/R)((t/R)+\phi)}, \qquad w_- = \phi - \frac{t}{R} - \frac{R r_+}{r^2 - r_+^2}, \qquad y = \frac{R}{\sqrt{r^2 - r_+^2}} e^{(r_+/R)((t/R)+\phi)}. \tag{4.8}$$

The periodicity of $\phi$ is equivalent to

$$w_+ \sim e^{4\pi^2 T_L} w_+, \qquad w_- \sim w_- + 2\pi, \qquad y \sim e^{2\pi^2 T_L} y. \tag{4.9}$$

The thermal entropy of the dual CFT is given by the standard formula $S_A = \frac{\pi^2}{3} c T_L$, and this agrees with the black hole entropy $S = 2\pi\sqrt{\frac{cL_0}{6}} = 2\pi\sqrt{Q_1 Q_5 N}$, using the thermodynamical relation $L_0 = \frac{\pi^2}{6} c T_L^2$.

### B. From near extremal BTZ to $AdS_2$

The near extremal 5D black hole is related to the near extremal BTZ black hole, $\frac{r_+ - r_-}{r_+} \ll 1$. In the dual CFT, the left-moving sector is far more excited compared with the right-moving sector, since $T_L \gg T_R$.

By considering the limit $r \to r_+$ of the BTZ metric (2.2), we define $u = r - r_+$ and assume $u \sim (r_+ - r_-) \ll r_+$. In the end we find the simplified metric

$$ds^2 = -\frac{4u(u + r_+ - r_-)}{R^2} dt^2 + \frac{R^2}{4u(u + r_+ - r_-)} du^2 + r_+^2 \left(\frac{dt}{R} + d\phi\right)^2. \tag{4.10}$$

The 2D part of (4.10) is equivalent to the "$AdS_2$ black hole" defined in [29],

$$ds^2 = -\frac{u(u + 4\pi Q^2 T_H)}{Q^2} dt^2 + \frac{Q^2}{u(u + 4\pi Q^2 T_H)} du^2, \tag{4.11}$$

where

$$Q^2 = \frac{R^2}{4}, \qquad T_H = \frac{r_+ - r_-}{\pi R^2}. \tag{4.12}$$

We can show that this space is equivalent to the pure $AdS_2$ via a coordinate transformation [29]. Though the temperature dependence disappears by this transformation, it reflects the choice of different thermal vacua [29]. Thus the 3D background (4.10) is equivalent to $S^1$ fibration over $AdS_2$.

In order to have a sensible interpretation in terms of $AdS_2/CFT_1$, the geometry should include the boundary region of the $AdS_2$ dual to the UV limit of $CFT_1$. This is given by the region $u \gg R$. On the other hand, the approximation to get (4.10) assumes the condition $u \ll r_+$. Thus we have to require

$$R \ll r_+. \tag{4.13}$$

This means that we cannot neglect the excitation in the $S^1$ direction of the spacetime. However, we can still perform the Kaluza-Klein reduction and regard the theory as the one on $AdS_2$ with infinitely many Kaluza-Klein modes.

The generators[7] $l_0$, $l_{\pm 1}$ and $\bar{l}_0$, $\bar{l}_{\pm 1}$ of the isometry $SO(2,2) = SL(2,R)_L \times SL(2,R)_R$ of the $AdS_3$ in the Poincare coordinate (4.4) are given by

$$l_{-1} = -\partial_{w_+}, \qquad l_0 = -(w_+ \partial_{w_+} + \tfrac{1}{2} y \partial_y), \qquad l_1 = -(w_+^2 \partial_{w_+} + w_+ y \partial_y - y^2 \partial_{w_-}), \tag{4.14}$$

and their antiholomorphic counterparts are obtained by exchanging $w_\pm$ with $w_\mp$. For states dual to generic BTZ black holes, the two $SL(2,R)$ symmetries are both broken. However, if we take the limit $R \to 0$ [i.e. (4.13)] of the extremal BTZ $r_+ = r_-$, we can keep $U(1)_L \times SL(2,R)_R$ (i.e. $l_0$ and $\bar{l}_{\pm 1}$, $\bar{l}_0$) unbroken as is clear from the orbifold action (4.9) on the expressions (4.14). The generator $U(1)_L$ is the translation in the $S^1$ direction, and the right-moving $SL(2,R)_R$ symmetry turns out to be essentially the same as the isometry of the $AdS_2$ [7].

This analysis of the conformal symmetry reveals that the excitation in the $S^1$ direction is related to the left-moving sector. Thus we can regard this $AdS_3/CFT_2$ as a variant of $AdS_2/CFT_1$ by treating the left-moving sector as an internal degree of freedom. Notice that excitations in the left-moving sector do not shift the value of the Hamiltonian for $CFT_1$ (i.e. $\bar{L}_0$). Thus the conformal quantum mechanics

[7]Notice that we distinguish $l_{0,\pm 1}$ from the standard basis $L_{0,\pm 1}$ dual to the Virasoro generators of 2D CFT. In our case, the unbroken generators of $l_{0,\pm 1}$ and $\bar{l}_{0,\pm 1}$ are linear combinations of the standard Virasoro generators.

dual to $AdS_2$ is essentially described by the right-moving part of $CFT_2$.

This suggests a discrete light-cone quantization (DLCQ) interpretation of the dual CFT. In order to properly normalize the metric (4.10) in the limit (4.13), we are led to define

$$X^+ = \frac{r_+}{R}\left(\frac{t}{R} + \phi\right), \qquad X^- = \frac{R}{r_+}\left(\frac{t}{R} - \phi\right). \tag{4.15}$$

Thus in this picture we can equivalently regard the $CFT_2$ as almost lightlike compactified $X^+ \sim X^+ + \frac{2\pi r_+}{R}$ and $X^- \sim X^- + \frac{2\pi R}{r_+}$. In this description, it is easy to confirm the unbroken $SL(2,R)$ symmetry because $w_-$ is scaled as $\frac{R}{r_+}w_-$ and gets insensitive under the orbifold action. Also, this rescaling shifts the energy scale we are looking at as $(p_+, p_-) \to (\frac{R}{r_+}p_+, \frac{r_+}{R}p_-)$. This agrees with the near extremal limit $L_0 \sim \frac{r_+}{R} \gg 1$ that we have been assuming so far. Notice also that in this limit the time evolution is equivalent to the one of the light-cone time $X^-$, and therefore the right-moving energy $\bar{L}_0$ is treated as the Hamiltonian.

### C. Two-point functions

In order to have a better understanding of the $AdS_2/CFT_1$ interpretation of the near extremal BTZ black hole, we would like to turn to the two-point function computed holographically following the bulk-to-boundary relation [35].

The Feynman Green function of a scalar field in global $AdS_3$ is given in [42] and, also, that in BTZ can be constructed by the orbifold method. $AdS_3$ is defined as the three dimensional hyperboloid $-x_0^2 - x_1^2 + x_2^2 + x_3^2 = -R^2$ embedded in $R^{2,2}$, and its metric takes the form $ds^2 = -dx_0^2 - dx_1^2 + dx_2^2 + dx_3^2$. In the global $AdS_3$, the Green function takes a fairly simple form, like

$$-iG_F(x,x') = \frac{1}{4\pi R}(z^2-1)^{-1/2}[z + (z^2-1)^{1/2}]^{1-2h_+}, \tag{4.16}$$

where

$$\begin{aligned} z &\equiv 1 + R^{-2}\sigma(x,x') + i\epsilon, \\ \sigma(x,x') &= \tfrac{1}{2}\eta_{\mu\nu}(x-x')^\mu(x-x')^\nu, \\ \eta_{\mu\nu} &= \mathrm{diag}(-1,-1,1,1). \end{aligned} \tag{4.17}$$

If we define the coordinate

$$\begin{aligned} x_0 &= \frac{y}{2}\left(1 + \frac{1}{y^2}(R^2 + w_+w_-)\right), & x_1 &= \frac{R}{2y}(w_+ - w_-), \\ x_2 &= \frac{y}{2}\left(1 - \frac{1}{y^2}(R^2 - w_+w_-)\right), & x_3 &= \frac{R}{2y}(w_+ + w_-), \end{aligned} \tag{4.18}$$

we obtain the Poincare coordinate (4.4). The parameter $z$ in the above coordinate becomes

$$z^{(\mathrm{Poincare})} = \frac{1}{2yy'}[y^2 + y'^2 + \Delta w_+ \Delta w_-], \tag{4.19}$$

and by substituting this in (4.16), we obtain the Green function in the Poincare coordinate.

Considering the images which come as a result of the orbifolding procedure, the Green function in the rotating BTZ becomes

$$\begin{aligned} -iG_{\text{nonext BTZ}}(x,x') = \frac{1}{4\pi R}\sum_{n=-\infty}^{\infty}(z_n^2-1)^{-1/2} \\ \times [z_n + (z_n^2-1)^{1/2}]^{1-2h_+}, \end{aligned} \tag{4.20}$$

$$\begin{aligned} z_n(x,x') - i\epsilon = \frac{1}{r_+^2 - r_-^2}\Bigg[\sqrt{r^2 - r_-^2}\sqrt{r'^2 - r_-^2}\cosh \\ \times\left(\frac{r_-}{R^2}\Delta t_n + \frac{r_+}{R}\Delta\phi_n\right) \\ + \sqrt{r^2 - r_+^2}\sqrt{r'^2 - r_+^2}\cosh \\ \times\left(\frac{r_+}{R^2}\Delta t_n - \frac{r_-}{R}\Delta\phi_n\right)\Bigg], \end{aligned} \tag{4.21}$$

where

$$\Delta t_n = t - t', \qquad \Delta\phi_n = \phi - \phi' + 2\pi n. \tag{4.22}$$

Now we would like to reduce the previous bulk-bulk Green functions to the $AdS_2$ ones. Notice that the geodesic length $z_n$ can always be taken to be very large since we can consider two points near the boundary of $AdS_2$ owing to (4.13). Thus the Green function looks like

$$G \sim \frac{1}{4\pi R}\sum_{n=-\infty}^{\infty}(z_n)^{-2h_+}. \tag{4.23}$$

Consider again the near extremal BTZ $\frac{r_+ - r_-}{r_+} \ll 1$ and take the limit $u = r - r_+ \gg R \sim r_+ - r_-$. Then we obtain

$$\begin{aligned} z_n &\sim \frac{\sqrt{yy'}}{r_+^2 - r_-^2}\left[\cosh\left(\frac{r_-\Delta t}{R^2} + \frac{r_+\Delta\phi_n}{R}\right)\right. \\ &\quad \left. - \cosh\left(\frac{r_+\Delta t}{R^2} + \frac{r_-\Delta\phi_n}{R}\right)\right] \\ &= 2\frac{\sqrt{yy'}}{r_+^2 - r_-^2}\sinh\left(\frac{(r_+ + r_-)}{2R}\left(\frac{\Delta t}{R} + \Delta\phi_n\right)\right) \\ &\quad \times \sinh\left(\frac{(r_+ - r_-)}{2R}\left(\frac{\Delta t}{R} - \Delta\phi_n\right)\right). \end{aligned} \tag{4.24}$$

In this case the holographic two-point function in the $AdS_2$ limit looks like (below we omit numerical constants)

$$\begin{aligned} \langle O(t,\phi)O(0,0)\rangle = \sum_n\Bigg[\sinh\left(\frac{(r_+ + r_-)}{2R}\left(\frac{\Delta t}{R} + \Delta\phi_n\right)\right) \\ \times \sinh\left(\frac{(r_+ - r_-)}{2R}\left(\frac{\Delta t}{R} - \Delta\phi_n\right)\right)\Bigg]^{-2h_+}. \end{aligned} \tag{4.25}$$

This takes the same expression as the one of the holographic two-point function of $CFT_2$ [43,44]. In the DLCQ coordinate, this is rewritten as follows:

$$\langle O(X^+, X^-)O(0,0)\rangle = \sum_n \Big[ \sinh\Big(X^+ + \frac{2\pi r_+}{R} n\Big) \times \sinh\Big(\frac{(r_+ - r_-)r_+}{2R^2} X^- + \pi n (r_+ - r_-)\Big)\Big]^{-2h_+}. \quad (4.26)$$

In the DLCQ coordinate, we treat $X^\pm$ as the basic coordinates, and thus in the scaling (4.13) we can set $n = 0$ in the above summation. Then the left- and right-moving sectors are decoupled as expected. Notice that the coordinate in the $S^1$ direction is $X^+$.

To interpret the near horizon limit of near extremal BTZ (i.e. $S^1$ fibration over $AdS_2$) from the viewpoint of the $AdS_2/CFT_1$, we need to regard the left-moving sector dual to the $S^1$ part as an internal degree of freedom, as we have explained before. This allows us to treat $X^+$ as a label of internal quantum number. Thus we can extract the two-point function of $CFT_1$ from (4.26) as follows:

$$\langle O(t)O(0)\rangle = [\sinh(\pi T_H t)]^{-2h_+}. \quad (4.27)$$

Here we have employed the relation $X^- \sim \frac{2}{r_+} t$, which is obtained from the infinite boost (4.15). This behavior agrees with the result for the thermal state in $AdS_2$ [29]. In particular, in the extremal limit $T_H \to 0$ we find

$$\langle O(t)O(0)\rangle = t^{-2h_+}, \quad (4.28)$$

as expected. In this way we have confirmed that we can regard the $AdS_3/CFT_2$ correspondence for the near extremal BTZ black hole equally as the $AdS_2/CFT_1$ with infinitely many internal degrees of freedom.

### D. Quantum entanglement and black hole entropy

As we have explained, the $AdS_3/CFT_2$ correspondence for the near extremal black holes can also be regarded as an $AdS_2/CFT_1$ by taking the near horizon limit of the near extremal BTZ black hole. Essentially, the $CFT_1$, i.e. the conformal quantum mechanics, is described by the right-moving sector of the original $CFT_2$ by treating the left-moving one as an internal degree of freedom tensored with the right-moving sector. When we consider the excitation in the $AdS_2$ spacetime with the $S^1$ sector untouched, the left-moving sector will always stay at $L_0 = N$, where $N$ is the quantized momentum in the original 5D black hole description.

Usually, the CFT dual of the rotating BTZ black hole is interpreted as a thermal state. Equally, we can interpret this as an entangled state in two copies of the same CFT [11],

$$|\Psi\rangle = \frac{1}{\sqrt{Z_0}} \sum_{n_L, n_R} e^{-\beta_L L_0/2 - \beta_R \bar{L}_0/2} (|n_L\rangle_L \otimes |n_R\rangle_R)_{\mathrm{CFT1}} \otimes (|n_L\rangle_L \otimes |n_R\rangle_R)_{\mathrm{CFT2}}, \quad (4.29)$$

where $Z_0 = \sum_{n_L, n_R} e^{-\beta_L L_0 - \beta_R \bar{L}_0}$ is the partition function of the 2D CFT. On the gravity side, they are geometrically understood as the CFTs living on the two disconnected boundaries of the BTZ spacetime.

To describe near extremal BTZ black holes, we keep $\beta_L$ finite and $\beta_R$ very large. In the near horizon limit $r \to r_+$, two boundaries of BTZ descend to the direct product of the two boundaries of $AdS_2$ times the circle $S^1$. We denote the states with $L_0 = N$ by $|k\rangle$ [$k = 1, 2, \cdots, d(N)$]. The number $d(N)$ of such states is very large, $d(N) \sim e^{2\pi\sqrt{Q_1 Q_5 N}}$. Then the quantum state looks like

$$|\Psi\rangle = \frac{1}{\sqrt{d(N)}} \sum_n \sum_{k=1}^{d(N)} e^{-\beta E_n/2} (|k\rangle_L \otimes |n\rangle_R)_{\mathrm{CFT1}} \otimes (|k\rangle_L \otimes |n\rangle_R)_{\mathrm{CFT2}}, \quad (4.30)$$

where $E_n = \langle n|\bar{L}_0|n\rangle$ is the energy of the CQM.

Consider the zero temperature limit $\beta = \infty$. Then the right-moving sector has a single ground state $|0\rangle$. The reduced density matrix of CQM1 $\rho_1$, which is obtained by tracing over CQM2, now becomes

$$\rho_1 = \frac{1}{\sqrt{d(N)}} \sum_{k=1}^{d(N)} |k\rangle\langle k|_{\mathrm{CQM1}}, \quad (4.31)$$

where $|k\rangle_{\mathrm{CQM1}} = |k\rangle_L \otimes |0\rangle_R$. This leads to the following entanglement entropy:

$$S_1 = \mathrm{Tr}[-\rho_1 \log \rho_1] = \log d(N) = 2\pi\sqrt{Q_1 Q_5 N}. \quad (4.32)$$

This clearly agrees with the familiar microscopic counting of BPS states, and thus is equal to the black hole entropy [6]. We can also confirm that it agrees with the entanglement entropy calculated holographically for the near horizon geometry $AdS_2 \times S^1 \times S^3 \times T^4$ of 5D (near) extremal black holes. In this way, we have shown that the $AdS_2/CFT_1$ description correctly reproduces the black hole entropy of (near) extremal 5D black holes.

We would like to stress that the density matrix (4.31) shows that the two quantum mechanics are maximally entangled. In general, it is possible to find a quantum state with a smaller value of entanglement entropy $S_1 < \log d(N)$, even if the number of degeneracy is $d(N)$. However, the entropy of extremal black holes known so far has always been explained by assuming maximally entangled states.

### E. Subtlety of the extremal limit

In this section we have mostly treated the extremal BTZ black holes as a limit of nonextremal ones, instead of starting with the extremal ones themselves. This is because

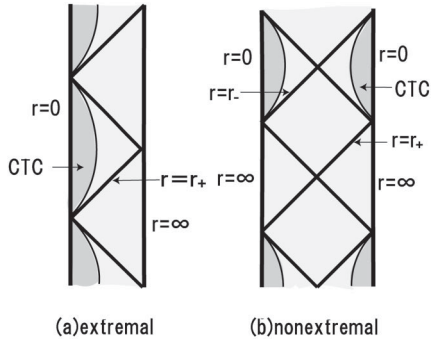


FIG. 4. The Penrose diagrams of the extremal and nonextremal BTZ black holes. There is a closed timelike curve in the shaded region.

the extremal limit sometimes looks subtle. This subtlety of defining extremal black hole entropy has been noticed for a long time [45].

First of all, this subtlety is noticed from the different forms of Penrose diagrams (Fig. 4) [41]. In both extremal and nonextremal cases, there are two boundaries in the Penrose diagram. Thus one may think that they should be interpreted as the two entangled CFTs. However, in the extremal case one of the two boundaries always includes the closed timelike curve [Fig. 4(a)], while in the nonextremal case it does not [Fig. 4(b)]. As far as we consider the nonextremal case, we can find the same boundary structure in the opposite boundary [as in Fig. 4(b)], and thus we can apply the interpretation[8] of two entangled CFTs [11,43,44,46–48].

In the extremal case, only one of the two boundaries has the sensible property with the CFT dual. Therefore, one may worry that the entangled interpretation is confusing in the strictly extremal case. On the other hand, most of the physical quantities of extremal black holes such as two-point functions are obtained smoothly from those of the nonextremal ones by taking the extremal limit $r_+ \to r_-$. Therefore, if we apply the previous analysis in the nonextremal case to the extremal case, we will get the same conclusion; the CFT dual to the extremal case is described by the entangled states. Refer also to the argument in [48] for an interesting candidate of a geometrical interpretation of these entangled pairs via $AdS_3/CFT_2$.

Even though we cannot completely resolve the mentioned conflict with the global geometry, the holographic consideration leading to (4.31) via $AdS_3/CFT_2$ tells us that the entangled interpretation is still correct even for strictly extremal black holes. Also notice that, in the near horizon limit $r \sim r_+$, we do not have to worry about this problem. This is because the near horizon geometry of the extremal case has no closed timelike curve, and two regular boundary CFTs are recovered in this limit. It will be an interesting future problem to explore this point.

[8]It is often claimed that we cannot extend the rotating black hole spacetime beyond the inner horizon [11,46,47]. Our derivation of black hole entropy from the holographic entanglement entropy done in Sec. II is still fine even if we take this restriction into account.

## V. FINITE SIZE CORRECTIONS OF ENTANGLEMENT ENTROPY AT FINITE TEMPERATURE

In this section we compute the entanglement entropy of a 2D free Dirac fermion at finite temperature when the spatial direction is compactified (to unit radius). This is the first analytical result of the entanglement entropy for a finite size 2D CFT at finite temperature. In the case of either infinite size or zero temperature, the expression of entanglement entropy becomes very simple and takes the form of the central charge $c$ times a universal function as found in [23,24]. However, in our case, the entanglement entropy depends more sensitively on the theory we consider.

In section II, we have seen that the relation (2.4) is very important for the understanding of BTZ black hole entropy in $AdS_3/CFT_2$. This important relation between thermal entropy and entanglement entropy can only be explicitly shown in a finite size system. Indeed, the behavior of the entanglement entropy agrees with what we expect from the geometric picture obtained from the AdS/CFT explained in Sec. II. This supports our claim that the black hole entropy is interpreted as the entanglement entropy in the dual CFT.

### A. Two-point function of a compactified boson

To make calculations simple, we consider the entanglement entropy of a free Dirac fermion $\psi$. This fermion is bosonized into a scalar field $\varphi$ with the unit radius $R = 1$ as $\psi = e^{i\varphi}$. We assume the Euclidean 2D theory on a torus defined by $z \sim z + 1$ and $z \sim z + \tau$ since we are interested in a finite temperature theory with a finite size. In particular, when the period $\tau$ is pure imaginary, $\tau = i\beta$, the theory is at the temperature $\beta^{-1}$ and its spacial size is 1.

The primary operator $O_{(n,w)}$ denotes the one with the momentum $n$ and the winding $w$ such that the chiral dimension becomes $\Delta_{n,w} = \frac{1}{2}(\frac{n}{R} + \frac{wR}{2})^2$ and $\bar{\Delta}_{n,w} = \frac{1}{2}(\frac{n}{R} - \frac{wR}{2})^2$.

Its two-point functions are given by (see e.g. Sec. 12 in [49])

$$\begin{aligned}\langle O_{(n,w)}(z,\bar{z}) O_{(-n,-w)}(0,0)\rangle &= \left(\frac{2\pi\eta(\tau)^3}{\theta_1(z|\tau)}\right)^{2\Delta_{n,w}} \overline{\left(\frac{2\pi\eta(\tau)^3}{\theta_1(z|\tau)}\right)^{2\bar{\Delta}_{n,w}}} \\ &\times \frac{\sum_{m,l} q^{\Delta_{m,l}} \bar{q}^{\bar{\Delta}_{m,l}} e^{4\pi i(\alpha_{n,w}\alpha_{m,l} z - \bar{\alpha}_{n,w}\bar{\alpha}_{m,l}\bar{z})}}{\sum_{m,l} q^{\Delta_{m,l}} \bar{q}^{\bar{\Delta}_{m,l}}}, \end{aligned} \tag{5.1}$$

where $\alpha_{n,w} \equiv \frac{1}{\sqrt{2}}(\frac{n}{R} + \frac{Rw}{2})$ and $\bar{\alpha}_{n,w} \equiv \frac{1}{\sqrt{2}}(\frac{n}{R} - \frac{Rw}{2})$.

In particular, we are interested in a Dirac fermion, which is equivalent to the real boson at the radius $R = 1$. For example, the one-loop partition function $Z_{\rm bos}(R)$ is transformed as follows:

$$Z_{\rm bos}(R=1)|\eta(\tau)|^2 = \sum_{n,w} q^{(n+w/2)^2/2}\bar{q}^{(n-w/2)^2/2} = \frac{|\theta_2(0|\tau)|^2 + |\theta_3(0|\tau)|^2 + |\theta_4(0|\tau)|^2}{2}. \quad (5.2)$$

In this way the free boson partition function is decomposed into the four sectors (R, NS), (NS, NS), (NS, R), and (R,R), each corresponding to $\nu = 2, 3, 4, 1$ of the theta function $\theta_\nu$, as usual.

### B. Calculating entanglement entropy

In general, to compute the entanglement entropy, we first divide the total system into two subsystems, $A$ and $B$. In our setup, we define $A$ (or $B$) to be an interval with length $L$ (or $1 - L$) at a specific time. Next, we compute $\mathrm{Tr}(\rho_A)^N$, where $\rho_A$ is the reduced density matrix obtained by taking a trace of the density matrix $\rho$ over the subsystem $B$, i.e. $\rho_A = \mathrm{Tr}_B\rho$. This is usually possible by assuming $N$ is a positive integer. Then we analytically continue with respect to $N$. Finally we take the derivative of $N$ and obtain the entanglement entropy $S_A$ of the subsystem $A$,

$$S_A = -\frac{\partial}{\partial N}\log \mathrm{Tr}(\rho_A)^N \Big|_{N=1}. \quad (5.3)$$

We can calculate $\mathrm{Tr}(\rho_A)^N$ by employing the following formula which relates it to a product of two-point functions of twisted operators [9,50],

$$\mathrm{Tr}\,(\rho_A)^N = \prod_{k=-(N-1)/2}^{N-1/2} \langle \sigma_k(z,\bar{z})\sigma_{-k}(0,0)\rangle, \quad (5.4)$$

with the understanding of $z = L$.

We identify the twist operator $\sigma_k$ with the operator $O_{(0,(k/N))}$, which has the fractional winding number $w = \frac{2k}{N}$ so that the fermion $\psi = e^{i\varphi}$ picks up the phase $e^{\pm(2\pi i/N)}$ if it goes around the two end points 0 and $z$. By setting $z = L$, we find that the extra phase becomes

$$e^{4\pi i(\alpha_{n,w}\alpha_{m,l}z - \bar{\alpha}_{n,w}\bar{\alpha}_{m,l}\bar{z})} = e^{4\pi i(mk/N)L}. \quad (5.5)$$

Thus the two-point function (5.1) in the $\nu = 2, 3, 4$ sector of the fermion becomes

$$\langle \sigma_k(z,\bar{z})\sigma_{-k}(0,0)\rangle_\nu = \left|\frac{2\pi\eta(\tau)^3}{\theta_1(L|\tau)}\right|^{4\Delta_k}\frac{|\theta_\nu(\frac{kL}{N}|\tau)|^2}{|\theta_\nu(0|\tau)|^2}, \quad (5.6)$$

where $\Delta_k = \frac{k^2}{2N^2}$. Below we assume that $\tau = i\beta$ is pure imaginary except in Sec. V H.

Now the entanglement entropy can be found by applying (5.3) and (5.4) to (5.6). To make the presentation simpler, we divide the entropy into two parts,

$$S_A = S_1 + S_2, \quad (5.7)$$

where $S_1$ is the one from the first factor in the right-hand side of (5.6), while $S_2$ is from the second factor.

It is easy to calculate $S_1$ since the expression depends on $N$ only via the conformal dimension $\sum_k \Delta_k = \frac{c}{24}\times(N - 1/N)$ (in our model the central charge is given by $c = 1$). We obtain

$$S_1 = \frac{c}{3}\log\left|\frac{\theta_1(L|\tau)}{2\pi\eta(\tau)^3}\right|. \quad (5.8)$$

The exact expression suitable for the low temperature expansion is given by

$$S_1 = \frac{c}{3}\log\left|\frac{1}{\pi}\sin(\pi L)\prod_{m=1}^{\infty}\times\frac{(1-e^{2\pi iL}q^m)(1-e^{-2\pi iL}q^m)}{(1-q^m)^2}\right|, \quad (5.9)$$

where $q = e^{-2\pi\beta}$. The expression of high temperature expansion is obtained from the modular transformation as follows:

$$S_1 = \frac{c}{3}\log\left|\frac{\beta}{\pi}e^{-(\pi L^2/\beta)}\sinh\left(\frac{\pi L}{\beta}\right)\times\prod_{m=1}^{\infty}\frac{(1-e^{2\pi L/\beta}\tilde{q}^m)(1-e^{-2\pi L/\beta}\tilde{q}^m)}{(1-\tilde{q}^m)^2}\right|, \quad (5.10)$$

where $\tilde{q} = e^{-(2\pi/\beta)}$. Notice that this contribution satisfies

$$S_1(L) = S_1(1-L) = S_1(1+L). \quad (5.11)$$

Second, $S_2$ is given by

$$S_2 = -\frac{\partial}{\partial N}\sum_{k=-(N-1)/2}^{(N-1)/2}\log\left|\frac{\theta_\nu(\frac{kL}{N}|\tau)}{\theta_\nu(0|\tau)}\right|^2\Big|_{N=1}. \quad (5.12)$$

In order to perform an analytical continuation with respect to $N$, we need to complete the summation of $k$. This can be done by expanding the logarithm in (5.12) explicitly by employing the standard formula $\log(1+x) = \sum_{l=1}^{\infty}\frac{(-1)^{l-1}}{l}x^l$, as we will see in the next subsection.

### C. High temperature expansion

We first restrict to the special case $\nu = 3$, i.e. the NS sector, for simplicity. We will come back to other spin structures in Sec. V G.

Let us evaluate $S_2$ in the high temperature expansion. In order to get the high temperature expansion, we need to perform the modular transformation $\tau \to -\frac{1}{\tau}$,

$$\frac{\theta_3(z|\tau)}{\theta_3(0|\tau)} = e^{-i\pi z^2/\tau}\cdot\frac{\theta_3(\frac{z}{\tau}|-\frac{1}{\tau})}{\theta_3(0|-\frac{1}{\tau})}. \tag{5.13}$$

Then we obtain

$$S_2 = -\frac{\partial}{\partial N}\sum_{k=-(N-1)/2}^{(N-1)/2}\left[-2\pi\frac{k^2L^2}{\beta N^2}\right]\Big|_{N=1} + \tilde{S}_2 = \frac{\pi}{3}\cdot\frac{L^2}{\beta} + \tilde{S}_2, \tag{5.14}$$

where the part $\tilde{S}_2$ is found to be

$$\begin{aligned}\tilde{S}_2 &= -2\frac{\partial}{\partial N}\sum_{k=-(N-1)/2}^{(N-1)/2}\sum_{m=1}^{\infty}\log\left[\frac{(1+e^{2\pi(kL/N\beta)}e^{-2\pi(m-1/2)/\beta})(1+e^{-2\pi(kL/N\beta)}e^{-2\pi(m-1/2)/\beta})}{(1+e^{-2\pi(m-1/2)/\beta})^2}\right]\Big|_{N=1}\\ &= -8\frac{\partial}{\partial N}\sum_{k=-(N-1)/2}^{(N-1)/2}\sum_{m=1}^{\infty}\sum_{l=1}^{\infty}\frac{(-1)^{l-1}}{l}\cdot\sinh^2\left(\frac{\pi kLl}{N\beta}\right)e^{-2\pi(m-1/2)(l/\beta)}|_{N=1}\\ &= -\sum_{l=1}^{\infty}\frac{(-1)^{l-1}}{l}\left[\frac{2\pi Ll}{\beta}\coth\left(\frac{\pi Ll}{\beta}\right)-2\right]\frac{1}{\sinh(\frac{\pi l}{\beta})}.\end{aligned} \tag{5.15}$$

In this calculation we have employed the following formula:

$$\frac{\partial}{\partial N}\sum_{k=-(N-1)/2}^{(N-1)/2}\sinh^2\left(\frac{\alpha k}{N}\right)\Big|_{N=1} = \frac{\partial}{\partial N}\left[-\frac{N}{2}+\frac{e^{(1-N)\alpha/N}-e^{(N+1)\alpha/N}}{2(1-e^{2\alpha/N})}\right]\Big|_{N=1} = -\frac{1}{2}+\frac{\alpha}{2}\coth\alpha. \tag{5.16}$$

In summary, the total expression of $S_A$ in the high temperature expansion becomes

$$\begin{aligned}S_A &= \frac{1}{3}\log\left[\frac{\beta}{\pi a}\sinh\left(\frac{\pi L}{\beta}\right)\right]+\frac{1}{3}\sum_{m=1}^{\infty}\log\left[\frac{(1-e^{2\pi(L/\beta)}e^{-2\pi(m/\beta)})(1-e^{-2\pi(L/\beta)}e^{-2\pi(m/\beta)})}{(1-e^{-2\pi(m/\beta)})^2}\right]\\ &\quad+2\sum_{l=1}^{\infty}\frac{(-1)^l}{l}\cdot\frac{\frac{\pi Ll}{\beta}\coth(\frac{\pi Ll}{\beta})-1}{\sinh(\pi\frac{L}{\beta})}.\end{aligned} \tag{5.17}$$

In this final expression, we make the dependence on the UV cutoff $a$ explicit. We plotted the function (5.17) in Fig. 5 by setting $a = \frac{1}{2\pi}$ and $\beta = 0.6$.

The first factor $\frac{1}{3}\log[\frac{\beta}{\pi a}\sinh(\frac{\pi L}{\beta})]$ reproduces the known result in the infinite size limit [24]. This part is successfully reproduced from the holographic dual computation in a BTZ black hole via AdS/CFT in [9].

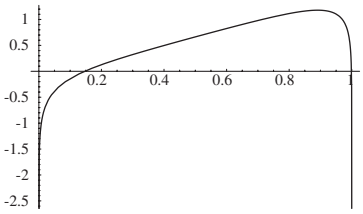


FIG. 5. The entanglement entropy as a function of $L$ when $\beta = 0.6$. We get rid of the divergence due to the cutoff by setting $a = \frac{1}{2\pi}$. We observe an approximately linear increase of the entropy as $L$ becomes large, assuming $L$ is not close to the values $L = 0, 1$. This is essentially due to the thermal contribution to the entanglement entropy.

By taking the limit $\epsilon = 1 - L \to 0$, we find

$$\begin{aligned}S_A(L=1-\epsilon) &= \frac{1}{3}\log\epsilon+\frac{\pi}{3\beta}+\sum_{l=1}^{\infty}\frac{(-1)^l}{l}\\ &\quad\times\left[\frac{2\pi l}{\beta}\coth\left(\frac{\pi l}{\beta}\right)-2\right]\frac{1}{\sinh(\frac{\pi l}{\beta})}.\end{aligned} \tag{5.18}$$

Thus we can extract the finite part

$$\begin{aligned}S(1)_{\text{finite}} &\equiv S(1-\epsilon)-S(\epsilon)\\ &= \frac{\pi}{3\beta}+\sum_{l=1}^{\infty}\frac{(-1)^l}{l}\left[\frac{2\pi l}{\beta}\coth\left(\frac{\pi l}{\beta}\right)-2\right]\frac{1}{\sinh(\frac{\pi l}{\beta})}.\end{aligned} \tag{5.19}$$

Clearly, the leading term $\frac{\pi}{3\beta}$ represents the thermal entropy in the high temperature limit $\beta \to 0$.

On the other hand, the full expression of thermal entropy $S_{\text{thermal}}$ is given by

$$S_{\text{thermal}} = -\frac{\partial F}{\partial T} = \beta^2 \frac{\partial}{\partial \beta}[-\beta^{-1}\log Z]$$
$$= \frac{\pi}{3\beta} + 4\sum_{m=1}^{\infty}\log(1+e^{-(2\pi/\beta)(m-(1/2))}) - \frac{8\pi}{\beta}\sum_{m=1}^{\infty}\frac{m-\frac{1}{2}}{e^{(2\pi/\beta)(m-(1/2))}+1}, \quad (5.20)$$

where the partition function $Z$ is defined by

$$Z = \frac{|\theta_3(0|\tau)|^2}{|\eta(\tau)|^2} = \frac{|\theta_3(0|-\tau^{-1})|^2}{|\eta(-\tau^{-1})|^2} = e^{\pi/6\beta}\prod_{m=1}^{\infty}(1+e^{-(2\pi/\beta)(m-(1/2))})^4. \quad (5.21)$$

Remarkably, we can show that the total expression of (5.19) indeed agrees[9] with the thermal entropy $S_{\text{thermal}}$ for arbitrary $\beta$,

$$S(1)_{\text{finite}} = S_{\text{thermal}}. \quad (5.22)$$

This relation is very clear in the holographic picture based on AdS/CFT, as will be explained in Sec. II B.

### D. Low temperature expansion

On the other hand, it is possible to perform the low temperature expansion with the modular transformation undone. In the end, we obtain, similarly to (5.15),

$$S_2 = -2\frac{\partial}{\partial N}\sum_{k=-(N-1)/2}^{(N-1)/2}\sum_{m=1}^{\infty}\log\left[\frac{(1+e^{2\pi i(kL/N)}e^{-2\pi\beta(m-1/2)})(1+e^{-2\pi i(kL/N)}e^{-2\pi\beta(m-1/2)})}{(1+e^{-2\pi\beta(m-1/2)})^2}\right]\Bigg|_{N=1}$$
$$= 2\sum_{l=1}^{\infty}\frac{(-1)^{l-1}}{l}\cdot\frac{1-\pi lL\cot(\pi Ll)}{\sinh(\pi l\beta)}. \quad (5.23)$$

In summary, the total expression of entanglement entropy in the low temperature expansion becomes

$$S_A = \frac{1}{3}\log\left[\frac{1}{\pi a}\sin(\pi L)\right] + \frac{1}{3}\sum_{m=1}^{\infty}\log\left[\frac{(1-e^{2\pi iL}e^{-2\pi\beta m})(1-e^{-2\pi iL}e^{-2\pi\beta m})}{(1-e^{-2\pi\beta m})^2}\right] + 2\sum_{l=1}^{\infty}\frac{(-1)^{l-1}}{l}\cdot\frac{1-\pi lL\cot(\pi Ll)}{\sinh(\pi l\beta)}. \quad (5.24)$$

At zero temperature, the formula (5.24) is simply reduced to

$$S_A = \frac{c}{3}\log\left[\frac{1}{\pi a}\sin(\pi L)\right], \quad (5.25)$$

and this reproduces[10] the known result [24]. This part is successfully reproduced from the holographic dual computation via AdS/CFT in [9].

Still one may worry if there are many poles which come from the final term in (5.24). However, this turns out to be an artifact of the order of the summation, as we will see in the next subsection. The high and low temperature expansion will be proved to be equivalent as they should be. The high temperature expression is suitable for numerical computations.

[9]This proof is elementary.

[10]Remember that we assume the space coordinate is compactified on a circle whose length is 1.

### E. Comparison of high and low temperature expansions

Originally, the low and high temperature expressions of entanglement entropy come from the same two-point function (via the modular transformation), and thus they are at least formally equivalent. However, as we have mentioned, they do not appear to be so at first sight.

In spite of this, we can show that, when they are expanded with respect to the powers of $L$ like

$$S_H = \sum_{n=1}^{\infty}C_n^H(\beta)L^{2n}, \qquad S_L = \sum_{n=1}^{\infty}C_n^L(\beta)L^{2n}, \quad (5.26)$$

coefficients match order by order, i.e. $C_n^H(\beta) = C_n^L(\beta)$. The point is the order of summation.

Let us present the proof of the equivalence. By applying the series expansions ($B_r$ are Bernoulli numbers),

$$1-\frac{x}{2}\cot\frac{x}{2} = \sum_{r=1}^{\infty}\frac{B_r}{(2r)!}x^{2r}, \qquad \frac{x}{2}\coth\frac{x}{2}-1 = \sum_{r=1}^{\infty}\frac{B_r(-1)^{r-1}}{(2r)!}x^{2r}, \quad (5.27)$$

to (5.17) and (5.24), the equalities $C_n^H(\beta) = C_n^L(\beta)$ are rewritten as follows:

$$\frac{\pi}{3\beta}+\frac{2\pi^2}{3}\sum_{l=1}^{\infty}\frac{(-1)^l\cdot l}{\beta^2\sinh\frac{\pi l}{\beta}} = \frac{2\pi^2}{3}\sum_{l=1}^{\infty}\frac{(-1)^{l-1}\cdot l}{\sinh(\pi l\beta)},$$
$$\sum_{l=1}^{\infty}\frac{(-1)^{l+n-1}\cdot l^{2n-1}}{\beta^{2n}\sinh\frac{\pi l}{\beta}} = \sum_{l=1}^{\infty}\frac{(-1)^{l-1}\cdot l^{2n-1}}{\sinh(\pi l\beta)} \qquad (n\geq 2). \quad (5.28)$$

These are equivalent to the relations

$$F_1(x) = -F_1\left(\frac{1}{x}\right) + \frac{1}{2\pi}, \quad F_n(x) = (-1)^n F_n\left(\frac{1}{x}\right) \quad (n \geq 2), \tag{5.29}$$

where we defined

$$F_n(x) = \sum_{l=1}^{\infty} (-1)^{l-1} l^{2n-1} \frac{x^n}{\sinh(\pi l x)}. \tag{5.30}$$

They can be proven by considering the integral representation

$$F_n(x) = \frac{1}{2\pi i} \oint_C dz \frac{-\pi x^n z^{2n-1}}{\sinh(\pi x z)\sin(\pi z)}, \tag{5.31}$$

where $C$ represents the path $z \in [-\infty + i\epsilon, \infty + i\epsilon] \cup [\infty - i\epsilon, -\infty - i\epsilon]$ (Fig. 6). It is easy to show (5.30) by summing over the residues of poles $z \in \mathbf{Z}$.

By deforming $C$ into $C'$, which surrounds the poles on the imaginary axis $z \in \frac{i}{x}\mathbf{Z} \neq 0$, we can indeed prove (5.29) directly (only when $n = 1$, we need to take into account the pole at $z = 0$).

In this way we have found that the low and high temperature expansions are equivalent. For the actual computation the high temperature expansion is more useful.

### F. Generalization

Here we would like to generalize the above result to the case in which the interval $A$ extends not only in the spacial direction but also in the temporal direction by setting $z = L + iT$, where $T$ is the Euclidean time. We also treat $\tau = \alpha + i\beta$ as a general complex number so that it includes the rotating black holes after the Lorentzian continuation. Remarkably, the entanglement entropy, like the thermal entropy, is expressed as the sum of the holomorphic contribution and the antiholomorphic one.

Generalization is straightforward since we only have to replace $i\beta \to \tau = \alpha + i\beta$ and $L \to z = L + iT$ in the previous results. The two-point function of twist operators becomes

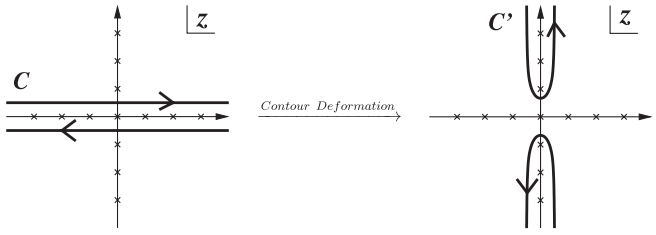


FIG. 6. We can compute the expression (5.31) in two ways, the original contour $C$ shown in the left figure and the deformed contour $C'$ shown in the right figure. The existence of the pole $z = 0$ should be taken into account only for the $n = 1$ case.

$$\langle \sigma_k(z,\bar{z})\sigma_{-k}(0,0)\rangle = \left|\frac{2\pi\eta(\tau)^3}{\theta_1(z|\tau)}\right|^{4\Delta_k} \frac{\theta_\nu(\frac{k}{N}z|\tau)\overline{\theta_\nu(\frac{k}{N}z|\tau)}}{|\theta_\nu(0|\tau)|^2}. \tag{5.32}$$

In the following calculation, we restrict to $\nu = 3$ as above.

We first evaluate $S$ in the high temperature expansion. $S_1$ is

$$\begin{aligned} S_1 &= \frac{1}{6}\log\left[-\frac{i\tau}{2\pi} e^{-(\pi i z^2/\tau)} \frac{\theta_1(\frac{z}{\tau}|-\frac{1}{\tau})}{\eta(-\frac{1}{\tau})^3}\right] + (\text{c.c.}) \\ &= \frac{1}{6}\left[\frac{\pi z^2}{i\tau} + \log\left[-\frac{i\tau}{\pi}\sin\left(\frac{\pi z}{\tau}\right)\right] + (\cdots)\right] + (\text{c.c.}), \end{aligned} \tag{5.33}$$

where $\cdots$ represents

$$(\cdots) = \sum_{m=1}^{\infty} \log\left[\frac{(1 - e^{2\pi i z/\tau}\tilde{q}^m)(1 - e^{-2\pi i z/\tau}\tilde{q}^m)}{(1-\tilde{q}^m)^2}\right], \tag{5.34}$$

with $\tilde{q} = e^{-2\pi i/\tau}$, and (c.c.) is the complex conjugate of the first term which comes from the antiholomorphic part. $S_2$ is calculated as

$$S_2 = -\left[\frac{\pi}{6i}\frac{z^2}{\tau} + \sum_{l=1}^{\infty} \frac{(-1)^{l-1}}{l} \frac{\frac{i\pi l z}{\tau}\coth(\frac{i\pi l z}{\tau}) - 1}{\sinh(\frac{i\pi l}{\tau})}\right] + (\text{c.c.}). \tag{5.35}$$

As a result we have

$$\begin{aligned} S_A = \frac{c}{6}\Bigg[&\log\left[\frac{\tau}{\pi a i}\sin\left(\frac{\pi z}{\tau}\right)\right] \\ &+ \sum_{m=1}^{\infty}\log\left[\frac{(1 - e^{2\pi i z/\tau}\tilde{q}^m)(1 - e^{-2\pi i z/\tau}\tilde{q}^m)}{(1-\tilde{q}^m)}\right]\Bigg] \\ &- \sum_{l=1}^{\infty} \frac{(-1)^{l-1}}{l} \frac{\frac{i\pi l z}{\tau}\coth(\frac{i\pi l z}{\tau}) - 1}{\sinh(\frac{i\pi l}{\tau})} + (\text{c.c.}), \end{aligned} \tag{5.36}$$

where we made the cutoff $a$ explicit.

The expression of $S_A$ in the low temperature expansion is also given as

$$\begin{aligned} S_A = \frac{c}{6}\Bigg[&\log\left[\frac{1}{\pi a}\sin(\pi z)\right. \\ &\left.\times \prod_{m=1}^{\infty}\frac{(1 - e^{2\pi i z} q^m)(1 - e^{-2\pi i z} q^m)}{(1-q^m)^2}\right] \\ &+ \sum_{l=1}^{\infty} \frac{(-1)^l}{l} \frac{1 - \pi l z\cot(\pi l z)}{\sinh(i\pi l\tau)} + (\text{c.c.}), \end{aligned} \tag{5.37}$$

where $q = e^{2\pi i\tau}$. Here the first and second terms are contributions from the holomorphic part of $S_1$ and $S_2$, respectively.

### G. Other spin structures

It is also useful to find the entanglement entropy for other spin structures of the Dirac fermions. First consider the case of $\nu = 2$, i.e. the finite temperature theory with the periodic boundary condition ($R$ sector). To calculate the entanglement entropy in the high temperature expansion, we again apply the modular transformation and obtain (the other parts are the same as the $\nu = 3$ case)

$$\tilde{S}_2 = 2\sum_{l=1}^{\infty}\frac{1}{l}\frac{\frac{\pi Ll}{\beta}\coth\frac{\pi Ll}{\beta} - 1}{\sinh\frac{\pi Ll}{\beta}}. \tag{5.38}$$

In this case, the thermal entropy defined by (5.20) becomes

$$S_{\text{thermal}} = \frac{\pi}{3\beta} + 4\sum_{m=1}^{\infty}\log(1 - e^{-(2\pi/\beta)(m-(1/2))}) - \frac{8\pi}{\beta}\sum_{m=1}^{\infty}\frac{m-\frac{1}{2}}{e^{(2\pi/\beta)(m-(1/2))} - 1}, \tag{5.39}$$

and we can check that $S_{\text{finite}}(L = 1)$ agrees with this.

It is also possible to compute the entanglement entropy in the $\nu = 4$ case. This corresponds to the index calculation in the NS sector $\text{Tr}_{\text{NS}}(-1)^F$ and is not related to any realistic thermal distribution. In this case, similarly we obtain

$$\tilde{S}_2 = -\frac{\pi L}{\beta} + 2\log 2 + 4\pi\sum_{l=1}^{\infty}\frac{(-)^l\cdot L}{\beta(e^{(2\pi lL/\beta)} - 1)} + 4\sum_{l=1}^{\infty}\frac{(-)^l}{l}\cdot\frac{\frac{\pi Ll}{\beta}\coth\frac{\pi Ll}{\beta} - 1}{e^{2\pi l/\beta} - 1}. \tag{5.40}$$

In the $\beta \to \infty$ limit, (5.15) and (5.40) vanish, respectively. This implies the boundary condition in the thermal direction can be neglected in this limit, as expected. The thermal entropy is

$$S_{\text{thermal}} = 2\log 2 - \frac{2\pi}{3\beta} + 4\sum_{m=1}^{\infty}\log(1 + e^{-(2\pi m/\beta)}) - \frac{8\pi}{\beta}\sum_{m=1}^{\infty}\frac{m}{e^{2\pi m/\beta} - 1}, \tag{5.41}$$

and we can check that $S_{\text{finite}}(L = 1)$ agrees with this.

### H. Temporal entanglement entropy: Beyond the horizon

For simplicity, here we take $\tau = i\beta$, which corresponds to the case of nonrotating black holes. It is worthwhile to take some notice of the case in which $z = \Delta t - i\frac{\beta}{2}$ in the above generalization. The imaginary shift $t \to t - i\frac{\beta}{2}$ of the Lorentzian time takes us from one boundary to the other boundary [43,44] (see Fig. 7).

When $\beta$ is sufficiently small, using the high temperature expansion, we find

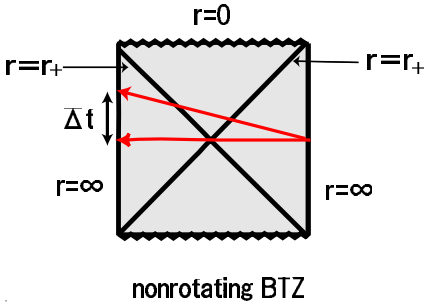


FIG. 7 (color online). The Penrose diagram of the nonrotating BTZ black hole. Red arrows stretching from one boundary to the other represent the geodesics between two boundaries, from which we compute a temporal analogue of entanglement entropy.

$$S_A \simeq \frac{c}{3}\log\left[\frac{\beta}{\pi a}\cosh\left(\frac{\pi\Delta t}{\beta}\right)\right]. \tag{5.42}$$

This entanglement entropy can be calculated also from the bulk geodesic point of view, since it is related to the bulk geodesic distance $|\gamma|$ between the points in which the twist operators are inserted [9] as in (2.1). The bulk geometry is the nonrotating BTZ black hole, and its Penrose diagram is shown in Fig. 7. The metric follows from (2.2) by taking $r_- = 0$ and $\beta = \frac{2\pi R^2}{r_+}$. The geodesic which corresponds to the above calculation can be seen in Fig. 7. Here we set $t = 0$ at the initial point. The geodesic distance can be exactly found [44],

$$|\gamma| = 2R\log\left[\frac{\beta}{\pi a}\cosh\left(\frac{\pi\Delta t}{\beta}\right)\right]. \tag{5.43}$$

Since the central charge is given by $c = \frac{3R}{2G_N^{(3)}}$ [51], we can precisely show the equality $S_{\text{ent}} = S_A$.

We see, as above, that the bulk and the boundary calculations are identical. Notice that the geodesic involved in the bulk computation now extends beyond the event horizon. Even though we have a definite definition of this temporal entanglement entropy in the Euclidean CFT, the physical meaning of this temporal entanglement entropy is not clear. It may be an analogue of the Polyakov loop in the context of Wilson loops. Further understandings of this quantity will deserve a future study.

## VI. CONCLUSION AND DISCUSSION

In this paper, we have explored the origin of black hole entropy from the viewpoint of AdS/CFT correspondence. We have been particularly interested in the black holes whose near horizon geometries include $\text{AdS}_2$. Extremal or near extremal black holes in 4D and 5D fall into this class. We argued that the $\text{AdS}_2/\text{CFT}_1$ correspondence leads to the equivalence between the black hole entropy and the von Neumann entropy associated with the quantum entanglement between a pair of quantum mechanical systems.

The remarkable fact that the $AdS_2$ space in the global coordinate has two timelike boundaries plays a crucial role in this quantum entanglement. This turns out to be the reason why we get nonzero entropy of extremal black holes, though its dual $AdS_2$ space is at zero temperature. This may be comparable to the entanglement interpretation for AdS black holes in higher dimensions considered in [11].

In summary, the mechanism of producing nonzero entanglement entropy is as follows. First, the BPS states in the internal spaces (such as Calabi-Yau spaces, $K3$ or $T^4$) produce a large degeneracy of ground states. Then the $AdS_2$ space, which has two boundaries, maximally entangles them, and in the end we obtain a large entanglement entropy which agrees with the black hole entropy.

There is a possibility that we have to restrict the physical spacetime to a certain region (e.g. outside the inner horizon [11,46,47]) in the global AdS. However, our derivation of entanglement entropy can still be applied without any change even in such a case, as long as there are two timelike boundaries. As we mentioned at the end of Sec. III, this may lead to a subtle issue in the strictly extremal black holes. Though we believe this is not a serious problem, the better understanding of this subtlety, as well as the precise derivation of the two-point functions (3.5) and (3.6) from the CQM side, will be important future problems.

In the latter part of this paper, we computed the entanglement entropy in the 2D free Dirac fermion theory. We obtained an analytical expression in the presence of both the finite size and finite temperature effect. This is the first analytical result of entanglement entropy in 2D CFT which takes both effects into account. Importantly, the result depends not only on the central charge of the CFT but also on many other details of the theory. This analysis enables us to show explicitly that the entanglement entropy is reduced to the thermal entropy when the subsystem $A$ becomes coincident with the total system. As we pointed out in Sec. II, this relation offers further evidence for the holographic computation of entanglement entropy found in [9], which also plays an important role in our discussions of $AdS_2/CFT_1$. It is also interesting to extend our results to a 2D free massless scalar field theory and eventually to the symmetric orbifold theories which have clear holographic duals.

## ACKNOWLEDGMENTS

We are extremely grateful to P. Calabrese, J. Cardy, V. Hubeny, M. Rangamani, A. Strominger, and Y. Tachikawa for very helpful comments on the draft of this paper and for important suggestions. T. T. would like to thank the High Energy Theory Group at Harvard University, where this work was finalized, for hospitality. The work of T. T. is supported in part by JSPS Grant-in-Aid for Scientific Research No. 18840027 and by JSPS Grant-in-Aid for Creative Scientific Research No. 19GS0219. The work of T. N. is supported by JSPS Grant-in-Aid for Scientific Research No. 19·3589.

[1] J. M. Maldacena, Adv. Theor. Math. Phys. **2**, 231 (1998); Int. J. Theor. Phys. **38**, 1113 (1999); O. Aharony, S. S. Gubser, J. M. Maldacena, H. Ooguri, and Y. Oz, Phys. Rep. **323**, 183 (2000).
[2] H. K. Kunduri, J. Lucietti, and H. S. Reall, Classical Quantum Gravity **24**, 4169 (2007).
[3] D. Astefanesei, K. Goldstein, R. P. Jena, A. Sen, and S. P. Trivedi, J. High Energy Phys. 10 (2006) 058.
[4] D. Astefanesei and H. Yavartanoo, arXiv:0706.1847.
[5] A. Strominger and C. Vafa, Phys. Lett. B **379**, 99 (1996).
[6] C. G. Callan and J. M. Maldacena, Nucl. Phys. **B472**, 591 (1996).
[7] A. Strominger, J. High Energy Phys. 01 (1999) 007.
[8] R. Britto-Pacumio, J. Michelson, A. Strominger, and A. Volovich, arXiv:hep-th/9911066.
[9] S. Ryu and T. Takayanagi, Phys. Rev. Lett. **96**, 181602 (2006); J. High Energy Phys. 08 (2006) 045.
[10] V. E. Hubeny, M. Rangamani, and T. Takayanagi, J. High Energy Phys. 07 (2007) 062.
[11] J. M. Maldacena, J. High Energy Phys. 04 (2003) 021.
[12] I. R. Klebanov, D. Kutasov, and A. Murugan, arXiv:0709.2140.
[13] T. Nishioka and T. Takayanagi, J. High Energy Phys. 01 (2007) 090.
[14] L. Bombelli, R. K. Koul, J. H. Lee, and R. D. Sorkin, Phys. Rev. D **34**, 373 (1986); M. Srednicki, Phys. Rev. Lett. **71**, 666 (1993).
[15] L. Susskind and J. Uglum, Phys. Rev. D **50**, 2700 (1994).
[16] T. M. Fiola, J. Preskill, A. Strominger, and S. P. Trivedi, Phys. Rev. D **50**, 3987 (1994).
[17] T. Jacobson, arXiv:gr-qc/9404039.
[18] S. Hawking, J. M. Maldacena, and A. Strominger, J. High Energy Phys. 05 (2001) 001.
[19] R. Emparan, J. High Energy Phys. 06 (2006) 012.
[20] R. Brustein, M. B. Einhorn, and A. Yarom, J. High Energy Phys. 01 (2006) 098.
[21] S. N. Solodukhin, Phys. Rev. Lett. **97**, 201601 (2006).
[22] M. Cadoni, Phys. Lett. B **653**, 434 (2007); arXiv:0709.0163;
[23] C. Holzhey, F. Larsen, and F. Wilczek, Nucl. Phys. **B424**, 443 (1994).
[24] P. Calabrese and J. Cardy, J. Stat. Mech. 06 (2004) P002; Int. J. Quantum. Inform. **4**, 429 (2006).
[25] D. V. Fursaev, J. High Energy Phys. 09 (2006) 018.
[26] M. Banados, C. Teitelboim, and J. Zanelli, Phys. Rev. Lett. **69**, 1849 (1992).

[27] J. M. Maldacena and A. Strominger, J. High Energy Phys. 12 (1998) 005.
[28] R. Dijkgraaf, J. M. Maldacena, G. W. Moore, and E. P. Verlinde, arXiv:hep-th/0005003.
[29] M. Spradlin and A. Strominger, J. High Energy Phys. 11 (1999) 021.
[30] D. Gaiotto, M. Guica, L. Huang, A. Simons, A. Strominger, and X. Yin, J. High Energy Phys. 03 (2006) 019.
[31] D. Gaiotto, A. Strominger, and X. Yin, J. High Energy Phys. 11 (2005) 017.
[32] F. Denef and G. W. Moore, arXiv:hep-th/0702146.
[33] J. M. Maldacena, J. High Energy Phys. 12 (1997) 002.
[34] C. Vafa, Nucl. Phys. **B463**, 435 (1996).
[35] S. S. Gubser, I. R. Klebanov, and A. M. Polyakov, Phys. Lett. B **428**, 105 (1998); E. Witten, Adv. Theor. Math. Phys. **2**, 253 (1998).
[36] J. M. Maldacena and L. Maoz, J. High Energy Phys. 02 (2004) 053.
[37] D. V. Fursaev and S. N. Solodukhin, Phys. Rev. D **52**, 2133 (1995).
[38] J. M. Bardeen and G. T. Horowitz, Phys. Rev. D **60**, 104030 (1999).
[39] R. M. Wald, Phys. Rev. D **48**, R3427 (1993); V. Iyer and R. M. Wald, Phys. Rev. D **50**, 846 (1994).
[40] T. Jacobson, G. Kang, and R. C. Myers, Phys. Rev. D **49**, 6587 (1994).
[41] M. Banados, M. Henneaux, C. Teitelboim, and J. Zanelli, Phys. Rev. D **48**, 1506 (1993).
[42] I. Ichinose and Y. Satoh, Nucl. Phys. **B447**, 340 (1995).
[43] S. Hemming, E. Keski-Vakkuri, and P. Kraus, J. High Energy Phys. 10 (2002) 006.
[44] P. Kraus, H. Ooguri, and S. Shenker, Phys. Rev. D **67**, 124022 (2003).
[45] S. W. Hawking, G. T. Horowitz, and S. F. Ross, Phys. Rev. D **51**, 4302 (1995).
[46] T. S. Levi and S. F. Ross, Phys. Rev. D **68**, 044005 (2003).
[47] V. Balasubramanian and T. S. Levi, Phys. Rev. D **70**, 106005 (2004).
[48] D. Marolf and A. Yarom, J. High Energy Phys. 01 (2006) 141.
[49] P. Di Francesco, P. Mathieu, and D. Senechal, *Conformal Field Theory* (Springer, New York, 1997), p. 890.
[50] H. Casini, C. D. Fosco, and M. Huerta, J. Stat. Mech. 07 (2005) P007; arXiv:0707.1300.
[51] J. D. Brown and M. Henneaux, Commun. Math. Phys. **104**, 207 (1986).